Pergamon

Biochemical Pharmacology, Vol. 49, No. 4, pp. 537–543, 1995.

0006-2952/95 $9.50 + 0.00

0006-2952(94)00446-3

MOLECULAR PROPERTIES AND MYOCARDIAL SALVAGE EFFECTS OF MORIN HYDRATE

TAI-WING WU,*†‡ KWOK-PUI FUNG,* LING-HUA ZENG,* JUN WU,* ANDREW HEMPEL,§ ARTHUR A. GREY‖ and NORMAN CAMERMAN§

*Department of Clinical Biochemistry, University of Toronto and The Toronto Hospital, Toronto, Ontario; §Department of Biochemistry and ‖Carbohydrate Research Centre, University of Toronto, Toronto; Ontario; and †Centre for Cardiovascular Research, The Toronto Hospital, Toronto, Ontario, Canada

(*Received* 13 *July* 1994; *accepted* 31 *August* 1994)

Abstract—Morin hydrate is a bioactive pigment found in yellow Brazil wood. Recently, we reported that morin hydrate prolongs the survival of three types of cells from the human circulatory system against oxyradicals generated *in vitro*. The protection excels that given by equimolar concentrations of ascorbate, mannitol, and Trolox. Here, we demonstrate that, *in vivo*, morin hydrate at 5 μmol/kg actually reduced by >50% the tissue necrosis in post-ischemic and reperfused rabbit hearts. Mechanistically, morin hydrate not only scavenges oxyradicals, but also moderately inhibits xanthine oxidase, a free-radical generating enzyme from the ischemic endothelium. Among other possibilities, morin hydrate appears to chelate some metal ions (e.g. Fe^{2+}) in oxyradical formation, although this needs to be examined further. Nuclear magnetic resonance (at 500 mHz) and electron-impact mass spectrometry also supported a molecular formula of $C_{15}H_{10}O_7$ for morin hydrate. Only by X-ray crystallography was it clearly revealed that there are two water molecules attached by intermolecular hydrogen bonds to a morin molecule. Also, the three rings of morin hydrate approach coplanarity. This conformation favours a delocalization of electrons after oxyradical reduction, making morin an effective antioxidant. Thus, we have documented some of the molecular properties and myocardial salvage effects of morin hydrate.

Key words: morin; molecular properties; myocardial salvage

Morin hydrate, [$C_{15}H_{10}O_7 \cdot 2H_2O$; 2-(2,4-dihydroxyphenyl)-3,5,7-trihydroxy-4*H*-1-benzopyran-4-one; morin] is a light yellowish pigment found in the wood of old fustic (*Chlorophora tinctoria*) [1]. Recent studies indicate that morin hydrate, a food preservative [1, 2], inhibits lipid peroxidation in micelles [3] and in rat liver microsomes [4]. In our laboratory, we have shown that morin hydrate protects rat hepatocytes against oxyradical-induced damage *in vitro* and the rat liver from ischemia-reperfusion injury [5]. Most recently, we observed that morin hydrate protects human erythrocytes, ventricular myocytes and saphenous vein endothelial cells better than ascorbate, Trolox, and mannitol *in vitro* [6]. These data provoked our interest in determining whether morin hydrate protects the myocardium *in vivo* and its plausible molecular basis of action. Among the techniques employed were an ischemia-reperfusion model described for rabbits [7, 8], NMR, electron-impact mass spectrometry (EI–MS), and X-ray crystallography.

MATERIALS AND METHODS

Materials. Unless otherwise stated, all chemicals (reagent grade) were supplied by the Sigma Chemical Co. (St. Louis, MO). Morin hydrate at 95% purity was obtained from the Aldrich Chemical Co. (Milwaukee, WI).

Structure analysis. The electron-impact mass spectra of morin hydrate were acquired using a VG-Analytical ZAB-SE instrument. The electron-impact conditions were: 70 eV, source temperature 200°, and 100 μA trap current. The sample was introduced into the vacuum by direct insertion probe.

Proton NMR was performed with a Varian Unity Plus 500 MHz NMR spectrometer. The proton NMR spectrum of morin was recorded at 25° in a DMSO-d_6 solution with tetramethylsilane added as the internal reference standard. All assignments were made by first-order analysis.

X-ray crystallographic analysis. Crystals of morin hydrate were obtained as thin yellowish needles from a 1:1 (v/v) methanol–water mixture. Space group and preliminary cell parameters were obtained from precession camera photographs. Refined cell parameters were obtained by diffractometer measurement of the angular parameters of 12 high-angle reflections, for which $40° \leq 2\theta \leq 60°$, and application of the least-squares method. Crystal data are: a = 7.991 (6), b = 25.409 (9), c = 7.123 (5) Å, β = 94.78 (7)°, V = 1441 Å^3, Z = 4 molecules per cell, space group $P2_1/c$.

A crystal of dimensions 0.3 × 0.8 × 0.1 mm was chosen for data collection on an automated four-circle diffractometer, utilizing copper K_a radiation

‡ Corresponding author: Dr. Tai-Wing Wu, Department of Clinical Biochemistry, Faculty of Medicine, University of Toronto, and Cardiovascular Research Division, The Toronto Hospital ES 3-404B, 200 Elizabeth St., Toronto, Ontario M5G 2C4, Canada. Tel. (416) 340-3261; FAX (416) 787-0039.

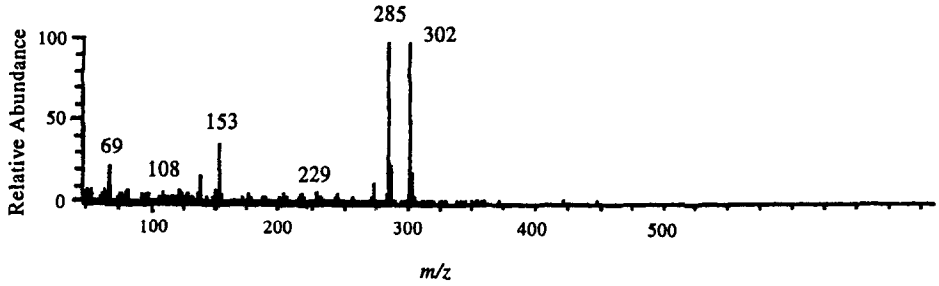

Fig. 1. Electron impact mass spectrum of morin.

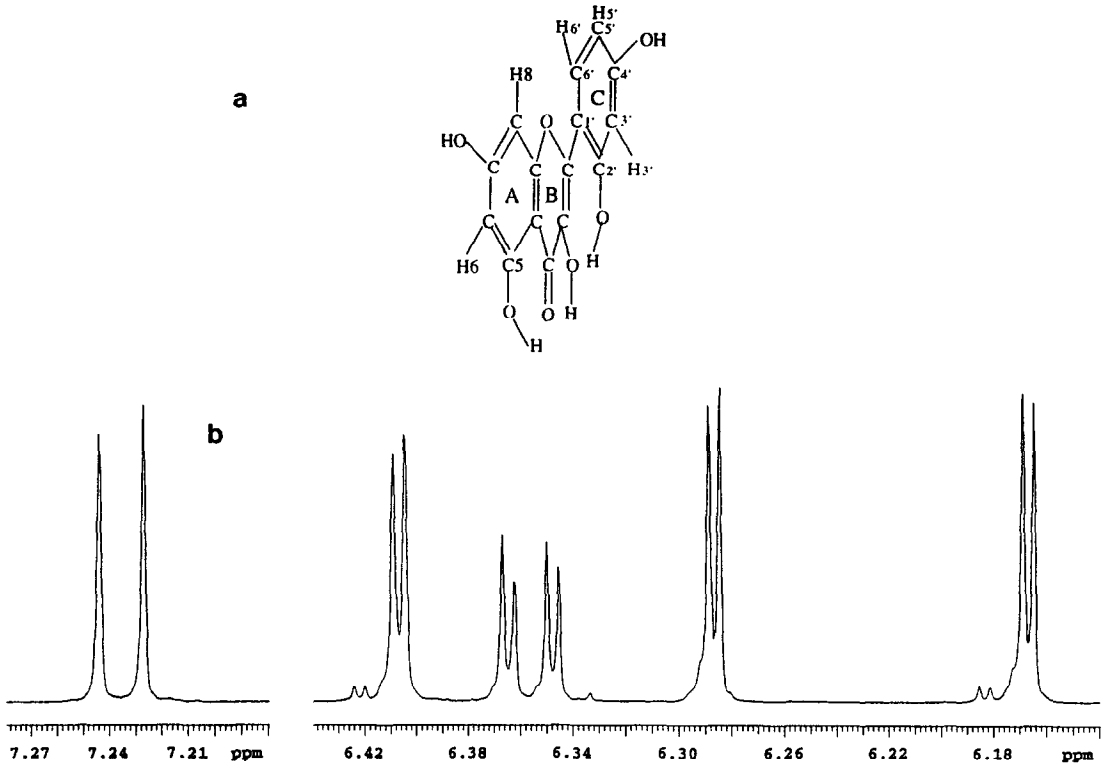

Fig. 2. (a) Chemical structure and (b) proton NMR spectrum of morin.

and θ:20 scan mode with scan speed of 2°/min. Three standard reflections monitored every 100 reflections showed only random variations within 5%. A total of 2450 unique reflections were recorded with $3° < 2\theta < 130°$ of which 1655 were considered observed using $F_o > 3\sigma$ (F_o) discrimination. The intensities were corrected for Lorentz and polarization factors. No absorption corrections were applied.

The crystal structure was determined by direct methods using the SHELXS-86 program; the resulting E-map revealed the positions of all nonhydrogen atoms in the structure.

Subsequent refinement and difference electron density calculations, using SHELXL-93, showed all hydrogen atoms and no other significant residual electron density. During refinement, the hydrogen atoms were maintained in their idealized positions. Positional parameters of hydrogen atoms at the two water molecules were free to vary. The refinement converged at a final discrepancy factor $R = 0.056$ and $S = 0.97$.

Ischemia-reperfusion. The same protocol as described previously [7] with minor modifications [8] was used. Note that this procedure had received ethical approval from the Toronto General Hospital Animal Care Committee. New Zealand white rabbits (3.0 to 3.5 kg) were injected intramuscularly with ketamine HCl (35 mg/kg) and Atravet (0.4 mg/kg). After shaving the frontal area of the neck and chest

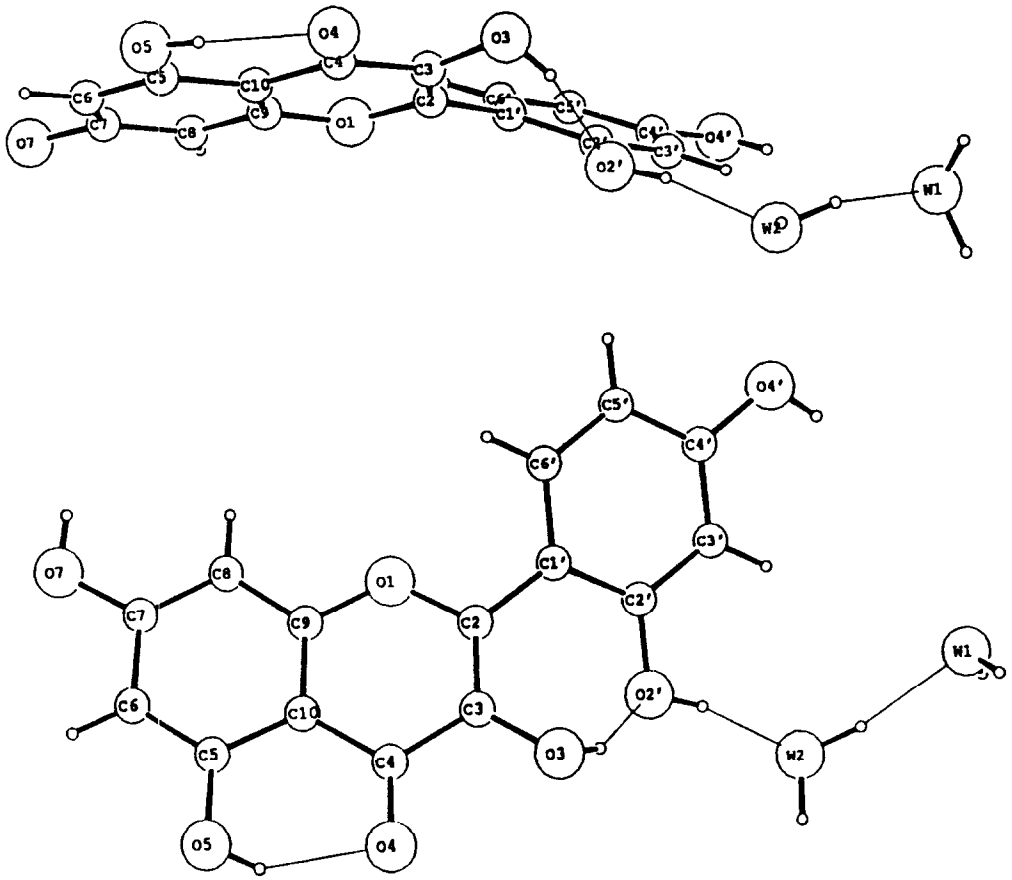

Fig. 3. X-ray crystallographic analysis of morin hydrate. (Bottom) Perpendicular to molecular plane. (Top) Parallel to molecular plane.

of the animal, anesthesia was maintained by tracheotomy and ventilating the animal with positive pressure respiration using a Harvard small animal respirator and a gas mixture of 2.5% enflurane (2-chloro-1,1,2-trifluoroethyl difluoromethyl ether) with O_2 (0.6 L/min). The right femoral artery was exposed and cannulated for measuring the arterial blood pressure and the right femoral vein for intravenous infusion of normal saline. Following a midline sternotomy, the pericardium was opened and the heart was exposed. A dose of 50 IU/kg of heparin sulfate was given intravenously via the ear vein. The main branch of the AVCA* that supplies much blood to the left ventricle and apex in the rabbit was ligated temporarily with a 5–0 silk thread for 1 hr at the site between $\frac{1}{2}$ to $\frac{1}{3}$ from apex to the atrioventricular groove. Attainment of ischemia was evidenced by the rapid change in colour of the left ventricle from red to pale purple, accompanied by marked elevations in the S-T segment of the electrocardiogram for the saline-infused control and the morin-infused hearts, but not in sham-operated controls. Approximately 2 min before releasing the occlusion, a 30-mL bolus of saline alone (placebo control) or with morin hydrate at 5 μmol/kg was injected into the animal through the right external jugular vein over ~5 min, followed by a 4-hr reperfusion. Note that the saline solution containing morin was sonicated for 15 min before use. Eight animals were used in randomized order for each permutation. In pilot experiments, we had noted that in control animals infused with saline before reoxygenation, neither the extent of myocardial necrosis in the area at risk, nor the percentage of area at risk alone, changed significantly ($P > 0.05$) whether reperfusion was 4 or 12 hr long.

After reperfusion, the heart was harvested, and the AVCA was ligated again. A 15-mL bolus of 0.25% Evans Blue in normal saline was infused into the heart via the aorta. In the area at risk (i.e. area previously made ischemic), there was no staining by Evans Blue. The heart was sliced transversely into 5–6 0.2-cm thick slices and incubated in 1.25% tetrazolium red for 25 min at 25°. No staining of the dye was found in the necrotic area, while in the non-necrotic area, a red stain developed [9]. Computerized planimetry was done on both surfaces of each slice as documented previously [10]. Further details concerning the protocol of this histochemical determination of percent necrosis/weight in rabbit myocardium, and its support by histopathology were

* Abbreviations: AVCA, anterior ventricular coronary artery; and XO, xanthine oxidase.

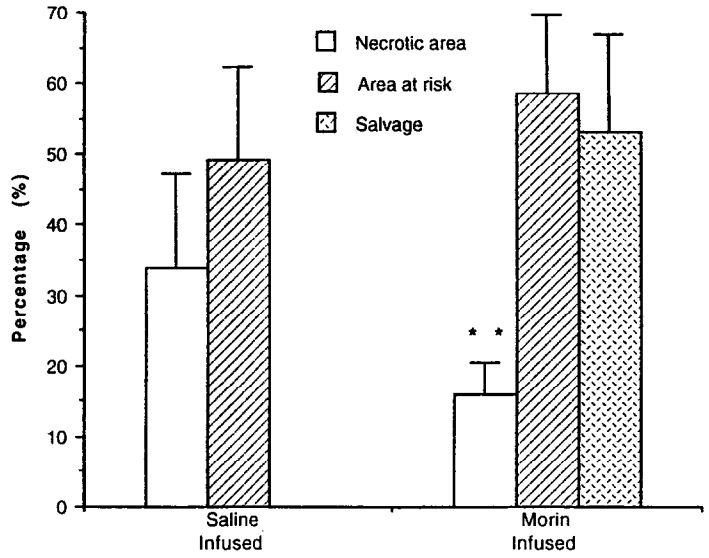

Fig. 4. Effect of morin on the salvage of the myocardium after ischemia–reperfusion in rabbits. Myocardial necrosis was obtained by infusion of saline (control) or 5 μmol morin hydrate in saline/kg into rabbits that underwent ischemia–reperfusion. Results are the means ± SD of 8 rabbits for each group. Key: (**) $P < 0.01$.

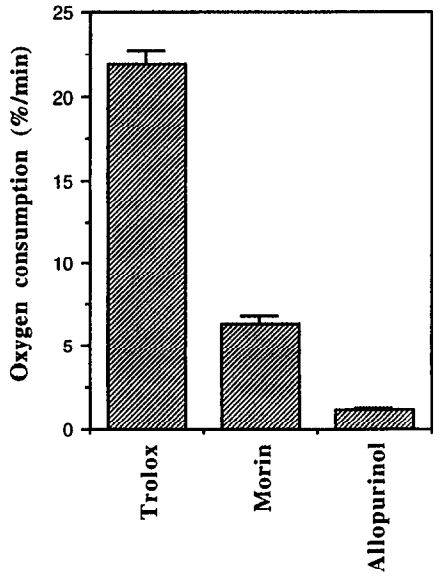

Fig. 5. Effect of morin hydrate, Trolox and allopurinol (each examined at 1 mM here) on the rate of oxygen uptake by XO. The rate of oxygen consumption in the reaction of XO with hypoxanthine was measured at 37° using a YSI Oxygen electrode [10]. After the first 30 sec, the consumption rate became highly linear and was measured in triplicate per permutation. Values are means ± SD.

as described previously [7, 8]. In this work, the region of tetrazolium positive-staining versus negative-staining (i.e. necrotic) myocardial tissue in the area at risk was also confirmed by transmission electron microscopy [7]. In our hands, we confirmed that the percentage of necrosis estimated gravimetrically (based on weight of necrotic tissue over total weight of slice) agreed within 5% with the determination of infarct size based on planimetry.

Inhibition of XO. This was assayed in two ways. The first method was based on the urate formed in the XO reaction with or without antioxidant added [11]. The antioxidant concentration that inhibited 50% of XO (IC_{50}) activity was recorded. In the second method, the rate of oxygen consumption in an oxygen electrode with and without antioxidant present was measured [10].

Detection of ferrous ion–morin hydrate complex. This was done according to Afanas'ev *et al.* [12]. Morin hydrate at 125 μM in PBS, pH 7.4, was mixed with an equimolar solution of $FeSO_4$ for 3 hr. Note that this incubation period was sufficiently long to form Fe^{2+}-morin hydrate complex. The absorption spectra of morin hydrate before and after forming the complex were recorded.

Statistical analysis. All data are expressed as means ± SD. Unless otherwise specified, statistical analysis was performed with the Statistical Analysis System Program (SAS Institute, Box 8000, Cary, NC, U.S.A.). Differences between groups were evaluated by analysis of variance (ANOVA), and the differences were specified by Duncan's multiple range test when the F value of the ANOVA was significant ($P < 0.05$).

RESULTS

In this work, the molecular structure and conformation of morin were borne out by its EI-MS (Fig. 1), proton NMR (Fig. 2), and X-ray

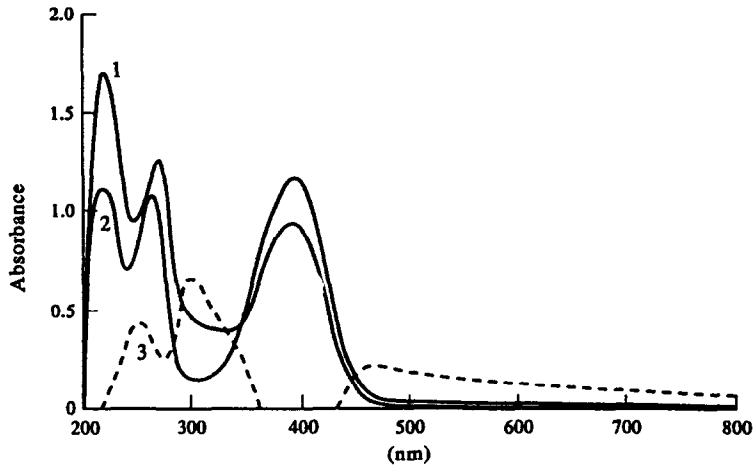

Fig. 6. Absorption spectra of morin hydrate and Fe^{2+}–morin hydrate complex at PBS, pH 7.4. This was done according to Afanas'ev *et al.* [12] (for details, see Materials and Methods). Curve 1 is the absorption spectrum of 62.5 μM morin hydrate against PBS, pH 7.4. Curve 2 is the differential spectrum of Fe^{2+}-morin hydrate against 62.5 μM $FeSO_4$ solution. The intensities of the maximum were the same at 390, 268 and 213 nm for curves 1 and 2. However, when Fe^{2+}–morin hydrate was recorded against 62.5 μM morin hydrate (curve 3), the differential spectrum contained new maxima at 460, 293 and 244 nm. The Fe^{2+}–morin hydrate complex was sufficiently stable, and its absorption spectrum did not change during the 18 hr. Note that the absorption spectra in this figure were obtained after 18 hr of incubation.

Table 1. IC_{50} values of morin hydrate, Trolox and allopurinol on XO

Antioxidant	IC_{50} (μM)
Morin hydrate	42.50 ± 6.87
Trolox	155.00 ± 14.40
Allopurinol	3.40 ± 0.81

The determination of IC_{50} values of antioxidants was performed according to Hall *et al.* [11]. Values are means ± SD; for each test, N = 4.

crystallography (Fig. 3). The positive ion EI-MS of morin (i.e. morin hydrate minus 2 water molecules) exhibited a molecular ion at m/z 302, fragment ions at m/z 285 (base peak, M-OH), 273 (M-HCO), 245 (M-HCO-CO), 229 (285–2CO), 153, 137, 108, and 69. The observed molecular and fragment ions are consistent with those in the proposed structure.

The NMR spectrum of morin in DMSO-d_6 at 25° (partially shown in Fig. 2b) is as follows: 12.591 ppm, 1H, s, OH; 10.647 ppm, 1H, br s, OH; 9.744 ppm, 1H, br s, OH; 9.52 ppm, 1H, very br s, OH; 9.01 ppm, 1H, very br s, OH; 7.234 ppm, 1H, d, $J5',6'$ = 8.51 Hz, H6'; 6.406 ppm, 1H, d, $J3',5'$ = 2.18 Hz, H3'; 6.355 ppm, 1H, dd, $J5',3'$ = 2.18, $J5',6'$ = 8.51 Hz, H5'; 6.285 ppm, 1H, d, $J6,8$ = 2.2 Hz, H8 or H6; 6.166 ppm, 1H, d, $J6,8$ = 1.91 Hz, H6 or H8 (Fig. 2b, hydroxy region not shown). All resonance patterns, chemical shifts and coupling constants are consistent with the proposed structure (Fig. 2a).

Four of the hydroxyl groups are broad, which suggests that these groups are in slow exchange with the H_2O from the DMSO solution. A two-dimensional-NOESY experiment supports this view since only correlation peaks from the OH resonances to the water peak could be observed. The sharp singlet at 12.591 ppm is probably involved in an intramolecular hydrogen bond. The hydroxyl group in question is probably that at the C5 position in ring A, which can interact with the acceptor carbonyl group at C4 in ring B (see Fig. 3 for atom numbering). Another hydrogen bond could involve the hydroxyl group at C2' on ring C, which theoretically could interact with either the furan oxygen in ring B or the hydroxyl oxygen at C3, depending on the orientation of ring C, or with a water molecule. The latter possibility is consistent with the crystal structure results.

The X-ray crystallographic configuration of morin is shown in Fig. 3. Two water molecules are attached to the morin molecule by intermolecular hydrogen bonds. The benzopyran ring system (ring A and B) is planar, and the angle between it and the phenyl ring plane (ring C) is approximately 30°; this configuration is stabilized by an intramolecular hydrogen bond between O3 (donor) and O2' (acceptor). Previous structure determinations of flavonoid compounds have yielded crystal conformations in which the ring systems range from nearly co-planar to nearly perpendicular [13], but none of these molecules have the inter-ring hydrogen bonding of morin and, therefore, are subject to freer rotation in solution.

The C2—C1' inter-ring bond in morin is slightly shorter and the O1—C2 and C3—C2 bonds slightly longer than similar bonds in 7-hydroxy-2',6'-

dimethoxyflavone [14], in which the angle between ring planes is 68°; thus, there may be some delocalization of electrons among the two ring systems in morin. In common with other hydroxyflavonoids, there is also an intramolecular H-bond from hydroxyl O5 to the neighboring carbonyl O4.

Figure 4 shows the effect of infusing 5 μmol/kg of morin hydrate in saline on the percent necrosis of the myocardium after 1 hr-ischemia, 4 hr-reperfusion in rabbits. The percent necrosis of the region at risk in the saline-treated group (N = 8) was 33.8 ± 13.5, while in the morin hydrate-treated group (N = 8) the extent of necrosis decreased significantly to 15.8 ± 4.6 ($P < 0.01$). Note that the areas at risk of both groups were statistically similar ($P > 0.05$), and negligible necrosis was observed in the sham-operated group (N = 6).

When the activity of XO was measured according to the method described by Hall *et al.* [11], we noted (Table 1) that the IC_{50} (concentration of morin that inhibited 50% of the initial rate of the enzyme) was 42.50 ± 6.87 μM (N = 4). This compares with the values of 155.00 ± 14.40 μM (N = 4) for Trolox (a vitamin E analogue) and 3.40 ± 0.81 μM (N = 4) for allopurinol. This trend was again shown (Fig. 5) when the rate of consumption of oxygen was monitored directly in a YSI electrode as referred to by us previously [10].

Morin hydrate has been known to form chelates and coloured complexes with a number of metal ions [1]. We have preliminary data supporting this contention. As exemplified in Fig. 6, the absorption spectra of morin hydrate did change before and after presumptive complexation with Fe^{2+}, and were sensitive to the duration and other conditions of incubation. Further spectroscopic studies are in progress.

DISCUSSION

In this study we have shown, in a rabbit model of myocardial infarct [7, 8], that an infusion of 5 μmol morin hydrate/kg immediately before reperfusion reduced by >50% the myocardial necrosis (Fig. 4). These data indicated that morin hydrate reduces the infarct size substantially. We have also observed (Wu T-W and Yang EC, unpublished data) a similar extent (approximately 60%) of reduction in blood malondialdehyde (a chemical marker of oxyradical damage) in the rabbit after our ischemia–reperfusion model. Therefore, apart from the evidence of infarct reduction based on tetrazolium staining supported by transmission electron microscopy, the malondialdehyde quantitation here has provided independent verification of the beneficial action by morin hydrate in reducing necrosis. In hemodynamic parameters, we have not detected any significant changes in pressure-rate index between the control and morin hydrate-infused animals during the ischemia-reperfusion period (data not shown).

While the reduction in experimental infarct size by morin hydrate was achieved, it was not known for certain if morin behaves as a free radical scavenger here, despite the popular belief that ischemia–reperfusion damage is oxyradical-based [15, 16]. At present, the sources of the presumptive free radicals in ischemia–reperfusion are not known for certain. For example, it has been suggested [15] that free radicals may arise from invading leukocytes, from injured mitochondria, and from oxidation of catecholamines. It also has been recognized that human and rabbit heart tissues are similar in their antioxidant defenses [17], hence our selection of the rabbit in our *in vitro* studies.

To obtain mechanistic insights into this issue, we investigated the stereochemical structure of morin hydrate via X-ray crystallography, the inhibitory effect of morin hydrate on XO, and the chelation property of morin hydrate with Fe^{2+}. From X-ray crystallography, we know that there is an intramolecular hydrogen bond between the ketone group on ring B and a hydroxy group on ring A (Fig. 3), and that this bonding may lower the aqueous solubility of MH (the maximal solubility of MH in water is approximately 1 mM). In this aspect, we may consider morin hydrate to be amphipathic—the free hydroxy groups on both rings enhance its solubility in water while the phenyl rings enhance its solubility in organic solvents. This property may facilitate the uptake of morin hydrate by the cell membrane, which contains both hydrophilic protein and hydrophobic lipid. We also know from the X-ray results that the intramolecular hydrogen bond from O3 to O2′ stabilizes the observed conformation, contributing to the partial aromatic character of the C2—C1′ bond.

Morin hydrate is a moderately potent inhibitor of XO. In two separate assays of XO activity it was shown (Fig. 5 and Table 1) that morin is distinctly more inhibitory of this enzyme than Trolox but less so than allopurinol. XO is a key enzyme, especially in the vascular endothelium in many organs. It can generate a cascade of oxyradicals when these organs undergo ischemia–reperfusion [15]. Our finding that morin hydrate can moderately inhibit XO implies that morin hydrate may act as a partially "preventive" antioxidant that militates against oxyradical generation, in addition to its ability to "cure" oxidative damage by scavenging oxyradicals. We also found that morin hydrate can form a metal (e.g. ferrous ion) complex (Fig. 6). We are studying the thermodynamics and kinetics of this complex formation between morin hydrate and metal ions. At present, it is not known what product(s) will be formed when morin hydrate interacts with oxyradicals *in vivo*. Presumably, this interaction may result in abstraction of a hydrogen atom from morin by the oxyradical. This type of one-electron transfer mechanism commonly takes place in other antioxidants including flavonoids [12]. The X-ray crystallographic analysis of the configuration of morin hydrate (Fig. 3) indicates that the resulting unpaired electron on morin can be stabilized by reconjugation of delocalized ring system (rings A and B are on the same plane, whereas the angle between rings A and B towards ring C is approximately 30°).

Taken together, this study strengthened our deduction that morin hydrate can effectively protect against oxyradical damage in rabbit heart during ischemia–reperfusion through multiple mechanisms. Morin may inhibit oxyradical generation by inhibiting

XO and/or chelating one or more metal ions such as Fe^{2+} in the cell or organ. It may also denote an electron to the oxyradical generated in the organ, forming a stable morin conjugated system. Further fundamental insights into the action of morin hydrate may permit us to better design or recognize other cardioprotectors of potential therapeutic value.

Acknowledgements—This work was supported in part, by a Heart and Stroke Foundation grant (A2688) to T.-W.W. The X-ray crystallography and NMR studies were supported by MRC grants (MT-4695 to N.C. and MA-6499 to A.A.G., respectively). We thank Dr. Henrianna Pang for help in executing the mass spectrometric analysis on morin and Mr. C. C. Yang for determining the inhibition constants on XO by various antioxidants.

REFERENCES

1. Windholz M, *The Merck Index*, 11th, Edn, pp. 986–987. Merck & Co., Rahway, NJ, 1989.
2. Smith C, Halliwell B and Aruoma OI, Protection by albumin against the pro-oxidant actions of phenolic dietary components. *Food Chem Toxicol* **30**: 483–489, 1992.
3. Wang PF and Zheng RL, Inhibition of the autoxidation of linoleic acid by flavonoids in micelles. *Chem Phys Lipids* **63**: 37–40, 1992.
4. Cholbi MR, Paya M and Alcaraz MJ, Inhibitory effects of phenolic compounds on CCl_4-induced microsomal lipid peroxidation. *Experientia* **47**: 195–199, 1991.
5. Wu T-W, Zeng LH, Wu J and Fung KP, Morin hydrate is a plant-derived and antioxidant-based hepatoprotector. *Life Sci* **53**: PL213–218, 1993.
6. Wu T-W, Zeng LH, Wu J and Fung KP, Morin: A wood pigment that protects three types of human cells in the cardiovascular system against oxyradical damage. *Biochem Pharmacol* **47**: 1099–1103, 1994.
7. Wu T-W, Wu J, Zeng LH, Sugiyama H, Mickle DA and Au JX, Reduction of experimental myocardial infarct size by infusion of lactosylphenyl Trolox. *Cardiovasc Res* **27**: 736–739, 1993.
8. Wu T-W, Zeng LH, Fung KP, Wu J, Pang H, Grey AA, Weisel RD and Wang JY, Effect of sodium tanshinone IIA sulfonate in the rabbit myocardium and on human cardiomyocytes and vascular endothelial cells. *Biochem Pharmacol* **46**: 2327–2332, 1993.
9. Jolly SR, Kane J, Bailie MN, Abrams GD and Lucchesi BR, Canine myocardial reperfusion injury: Its reduction by the combined administration of superoxide dismutase and catalase. *Circ Res* **54**: 277–285, 1984.
10. Wu T-W, Pristupa ZB, Zeng L-H, Au J-X, Wu J, Sugiyama H and Carey D, Enhancement in antioxidant-based hepatoprotective activity of Trolox by its conjugation to lactosylphenylpyranoside. *Hepatology* **15**: 454–458, 1992.
11. Hall IH, Scoville JP, Reynolds DJ, Simlot R and Duncan P, Substituted cyclic imides as potential anti-gout agents. *Life Sci* **46**: 1923–1927, 1990.
12. Afanas'ev IB, Dorozhko AI, Brodskii AV, Kostyuk VA and Potapovitch AI, Chelating and free radical scavenging mechanisms of inhibitory action of rutin and quercetin in lipid peroxidation. *Biochem Pharmacol* **38**: 1763–1769, 1989.
13. Cantrell JS, Crystal structures, bonding, and hydrogen bonding in flavonoid compounds. *Prog Clin Biol Res* **213**: 391–394, 1986.
14. Wallet J-C, Gaydou EM, Espinosa E, Osorno O, Molins E and Miravitlles C, Structure of 2-(2,6-dimethoxyphenyl)-7-hydroxy-4*H*-1-benzyopyran-4-one. *Acta Crystallogr* **C48**: 86–88, 1992.
15. Flaherty JT and Weisfeldt ML, Reperfusion injury. *Free Radic Biol Med* **5**: 409–419, 1988.
16. Ames BN, Shigenaga MK and Hagen TM, Oxidants, antioxidants, and the degenerative diseases of aging. *Proc Natl Acad Sci USA* **90**: 7915–7922, 1993.
17. Adachi T, Miura T, Noto T, Ooiwa H, Ogawa T, Tsuchida A, Iwamoto T, Goto M and Zimura O, Does verapamil limit myocardial infarct size in a heart deficient in xanthine oxidase? *Clin Exp Pharmacol Physiol* **17**: 769–779, 1990.